euspen's 20th International Conference & Exhibition, Geneva, CH, June 2020
www.euspen.eu

Diamond machining of optical functional surface

D. Li[1], Y. Zhang[1], X. Zhang[2], Dennis Neo[2], A. Davoudinejad[1], G. Tosello[1]

[1] *Technical University of Denmark, Department of Mechanical Engineering, DK-2800 Kgs. Lyngby, Denmark*
[2] *Singapore Institute of Manufacturing Technology, 71 Nanyang Drive, 638075, Singapore*

Email: dongyli@mek.dtu.dk

Abstract
Functional surfaces enabled by micro-/ Nano-structures have been investigated intensively in recent years. In the previous work, the authors managed to manufacture an optical functional surface on 2D/3D steel surfaces by micro milling. The surface function was to maximize the contrast introduced by the orthogonal textured anisotropic surfaces where the micro ridges worked as a micro mirror array. However, due to the severe tool wear of the mill, the geometry of the micro ridges was not finished perfectly [1]. The present paper reports a new process chain by utilizing diamond engraving to manufacture the same structures on the surface of RSA 905 with high accuracy. The manufacturing of the functional surface was conducted on an ultraprecision CNC machine. A 90° sharp tip tool were used for the shaping of the micro ridges. The tool path was programmed by Matlab and imported to the machine in the .NC format. A data matrix was used as an experimental object to test the optical functionality. Eight flat samples with different combinations of dimensions were produced to determine the machinability of the RSA 905 in terms of contrast generation. The optimal combination was the slope angle of 45° and the pitch of 50 µm. Moreover, the quantitative evaluation of the geometrical dimensions and the contrast of the microstructures was dedicated to the process optimization.

Keywords: Diamond machining, functional surface, contrast.

1. Introduction

Functional surfaces have been applied in a wide range of applications such as bio-engineering [1,2], chemical [3], optical [4] and mechanical production [5,6]. Diamond machining applied in the manufacturing of optical functional surface and the characterization of resultant surface quality were studied in depth. The works on the diamond machining of the radial Fresnel lens on roller moulds and the evaluation based on the surface roughness and 3D profile of the corresponding lens were reported by [7,8]. X. Zhang et al utilized diamond micro engraving to machine the gravure roller mould for roll-to-roll printing of fine line electronics and the application in real production [9]. E. Brinksmeier and L. Schonemann presented the application of the diamond micro chiseling to generate discontinuous microstructures and associated the surface finish with the structure size [10]. More generally, F. Z. Fang et al reported the state of art of the manufacturing and measurement of freeform optics where they discussed the applications and presented different manufacturing and characterization methods of varities of freeform surfaces [11].

In this paper, the surface functionality was the contrast generated by surfaces orthogonally textured with micro features. The contrast was generated by the anisotropic reflection led by the bevel surfaces of micro grooves. The surface quality of the micro bevels determined the reflection of the features. In the authors' previous works, such a functionality was successfully achieved on flat and cylinder surfaces of tool steel samples by micro milling [12,13].

This paper presents the evaluation of surface integrity of the surface with the optical functionality machined by diamond machining. A data matrix consisting of such micro grooves was patterned on RSA 905 samples for injection moulding. The surface integrity was evaluated by measuring the dimensions of the micro features, characterizing the burr formation and detection of possible defects left on the micro features that affect the surface functionality. The contrast generated by the microstructures was quantified by using a customized robotic measuring system for further optimization [12-14].

2. Experimental setup

2.1. Microstructures and the machine setup

Micro-grooves were used to achieve surface functions. The specific design is shown in **Figure 1**. In previous work [12], a similar structure was successfully patterned on the surface of tool steel by micro-milling. A sharp tool was used to cut the micro grooves on a mirror surface previously processed by a round tip tool. The desired anisotropic optical function was formed by the reflection of the micro structured surface: the light emitted by the light source at a fixed angle was reflected by the micro-machined surface to a direction, while the orthogonally textured surface reflected the light to other direction. Different brightness observed at a certain position was defined as the contrast.

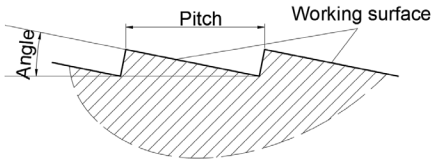

Figure 1. Micro ridges that define the surface anisotropical reflection.

In order to verify the function of this structure, a data matrix (text string "123456") was patterned on the samples used for micro injection molding as shown in **Figure 2.** The code on the metal sample was flipped. Corresponding to the black and white

modules in the figure, the black modules were cut vertically, while the white ones were processed horizontally or left blank.

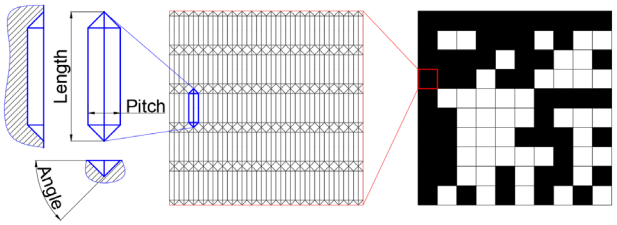

Figure 2. The hierarchy of a data matrix machined on the sample.

For comparison, micro structures with angles of 10 ° and 45 ° were machined. A module consisted of 100 (20 by 5) micro features where the pitch was 50 µm, angle was 44° and length was 200 µm. In addition, in order to get better reflcetion, the microstructures could be connnected to be continuous throughout the neighbour modules in the same color. In total, 8 samples numbered from "S1" to "S8" with different combination of features were machined, as shown in **Table 1.**

Table 1. Eight samples were machined with different combination of micro features.

Angle		45°		10°	
Continuous Features		No	Yes	No	Yes
White modules	Blank	*S1*	*S3*	*S5*	*S7*
	Horizontal	*S2*	*S4*	*S6*	*S8*

The experiments were performed on a Nanotech 350FG with a programming resolution and motion accuracy of 0.01 nm and 12.5 nm, respectively [15]. The setup in the machine is demonstrated in **Figure 3**.

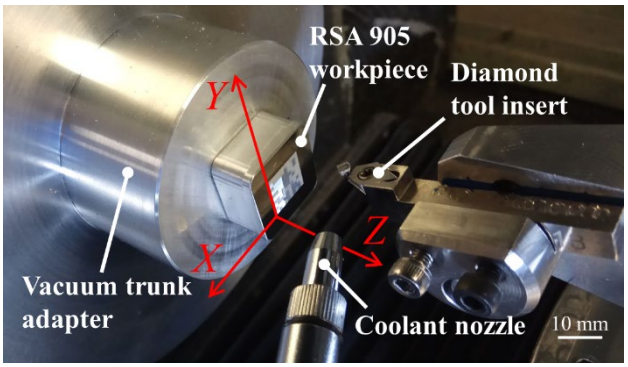

Figure 3. Setup in the machine.

Table 2. The specifications of the tools. [17]

Purpose	Shaping	Trimming
Tools	P90LEi	N0.50mLEi
Diamond type	Natural	Dodec synthetic
Tip shape	Sharp point	Round tip
Nominal tip radius [mm]	0	0.5
Included angle [°]	90	N.A.
Rake angle [°]	0	0
Clearance angle [°]	15	15

Two diamond insert tools (from Contour Fine Tooling, UK) were used in the two stages of processing: a round-tipped tool (N0.50mLEi) was used for trimming and a sharp-tipped tool (P90LEi) for the subsequent micro-structuring. The specifications of both tools are shown in **Table 2**. The work piece material was an injection moulding insert of RSA905 from RSP, the Netherlands [16]. Alcohol was used as the coolant to cool down the contacting zone and remove the chips from the sample surface. The feed speed was 150 mm/s in y- axis and depth of cut was around 3 µm, while other parameters were determined by the machine based on the tool path.

2.2. Tool path generation

In the experiments, due to the 15° clearance angle, see **Table 2**, the tool was tilted by 15°, in order to produce a cut-in angle of 30°, as indicated in the side view of **Figure 4**. The tool path was generated by defining the key points in Matlab. For a single micro groove, at least 5 points were necessary for defining the tool path: 4 points for the shape definition and 1 point for clearance. However, in a continuous machining, the tool moved from the end of the first to the start of the second groove that the two points overlapped. Moreover, in order to achieve better cutting condition, the depth of cut in this case was set to around 3 µm. Thus, the tool path was repeated at different position in z direction to achieve the desired depth: 24 µm for 44° grooves and 8.5 µm for 10° grooves.

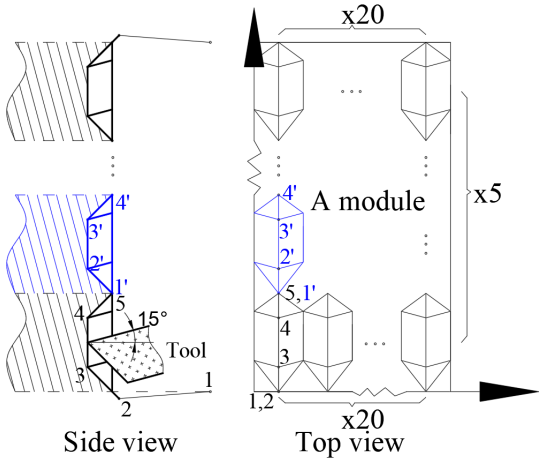

Figure 4. Tool path generation based on a module with discontinuous features.

2.3. Evaluation of surface quality

A confocal microscope Olympus Lext OLS 4100 was employed to measure the dimensions and the working surface roughness of the microstructures. 5 modules in the data matrix was selected randomly, and a 50x magnification lens was used to observe the center of each module. As shown in **Figure 5**, the 50x corresponded range of observation (258 x 258 µm^2) covered five micro grooves. The obtained images were post-processed using a software SPIP. Those parameters were extracted from the Lext images based on the cross section profile at three different positions of the micro features. The surface roughness of the slopes was characterized using Sa, the reason for which was the high consistency between the Sa and Sq from the measurements of this work.

Regarding the surface functionality, the contrast, a robotic-based platform (**Figure 6**) was developed to quantify the contrast of every module in the data matrix [14]. In this platform, a LED light source was fixed directly above the sample by a robot arm, while another robotic arm was used to move and rotate the camera about the sample. The sample was centered and aligned with the system coordinate. The position of the camera is defined by the angle between its axis and the z-axis of the system coordinate centered on the sample. Theoretically, during the measurement, the camera position could be tilted from the vertical position (0°) on the sample surface to 90°. However, due to the size of the robot and the camera, the starting point of

rotation was 10° for this system. The reflections of the black and white modules on the surface of the sample were extracted from the photos captured at various angles. The difference in exposure between the black and white module can be used to the quantify the contrast.

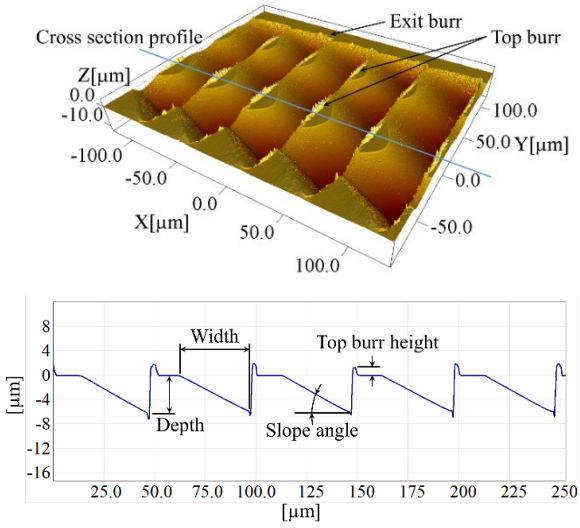

Figure 5. Geometrical measurement of micro features in SPIP® (higher aspect ratio applied for better visibility of the features).

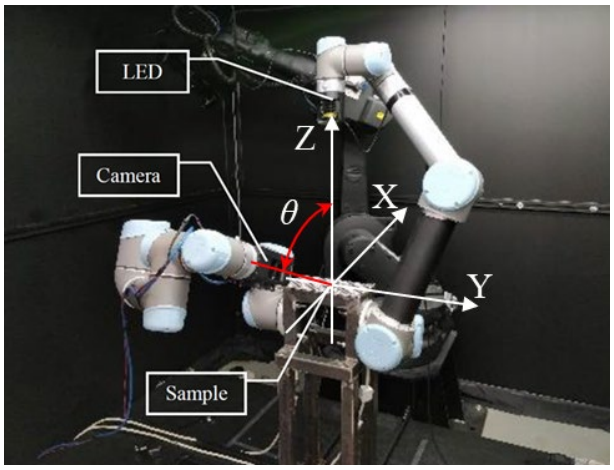

Figure 6. Customized robot-aided system for contrast evaluation.

3. Results and discussion

As shown in Figure 6, all eight samples can be successfully identified and read by a smart phone in general office scenes. At the same time, under different lighting conditions, the black and white colors could be reversed due to different reflection directions, such as S1 and S7 in **Figure 7**. The geometrical quality and the contrast samples were mearsured and analyzed using the evaluation methods described above.

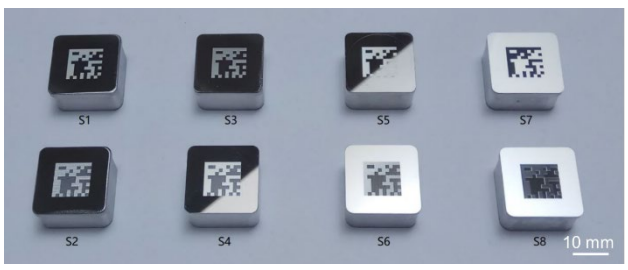

Figure 7. Eight samples with different combination of features by diamond machining.

3.1. Geometrical results

In this section, both 44° and 10° samples were considered: the width, depth, surface roughness, and burr formation were measured based on the 5 randomly selected modules. However, the microscope was not suitable for the surface roughness measurement on the 44° surface [18]. Only the surface roughness of the 10° structures was obtained in this study. Since the sampling modules were selected randomly, they were sorted according to the order in which each module was processed. The measured parameters were plotted in the same order, as shown in **Figure 8**. Only the results of S5 are presented in the figures. As indicated in **Section 2.2**, the width and the depth of the micro grooves were 48.58 ± 2.08 μm and 24.44 ± 2.35 μm, respectively, which was determined by the tool preset and geometry. The ratio k of the width to the depth was defined as **equation (1)**. The actual k was plotted against the groove number in **Figure 8 (a).** The slope anlges of the micro grooves were plotted against the module order in **Figure 8 (b).**

$$k = \frac{width}{depth} = \frac{50\ \mu m}{24.15\ \mu m} \approx 2.07 \qquad (1)$$

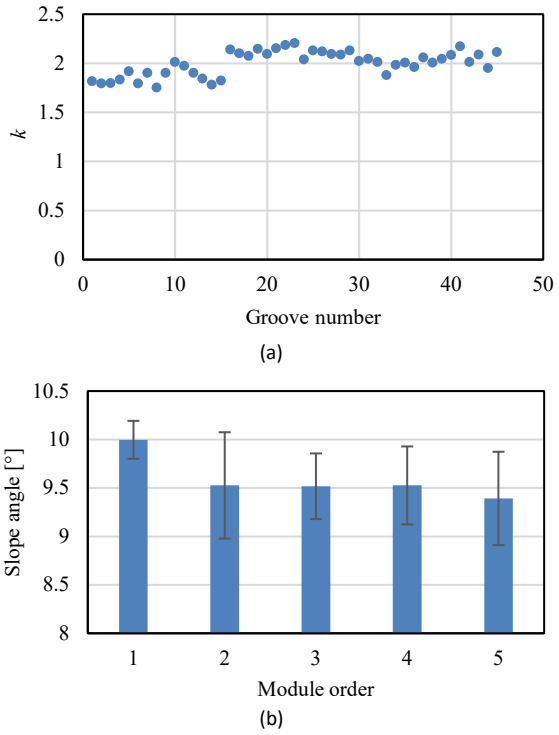

Figure 8. (a) Change trend of width to depth ratio among the micro grooves and (b) the average slope angle of the selected modules in the data matrix on S5.

As shown in **Figure 8 (a)**, the ratio between the width and the depth kept relatively constant around 2.07 with the processing. However, the variation of the two dimensions indicated the vibration in the z axis. The slope angle of the micro grooves decreased from 10° while the standard deviation indicated the distortion of the microslopes due to the vibration. Thus, in order to reduce the unstable dimensions, the tool path should be optimized to achieve smoother change in the corners. Moreover, the surface roughness of 10° grooves (Sa = 12 nm) and the burr height (h = 3.6 ± 1.2 μm) were disordered with the processing sequence of the modules.

3.2. Surface functionality

The contrast measurement of the sample using the above mentioned platform was mainly applied on the samples with 10° microstructures. That was due to that the optimal viewing angle for the light source set directly above the sample surface was 90°. However, it was not possible to obtain a valid and usable image to analyze the contrast of each module. Therefore, only the contrast measurement results of the 10° structure are presented. The average contrast between the black and white modules in the data matrix at various angles is shown in **Figure 9**.

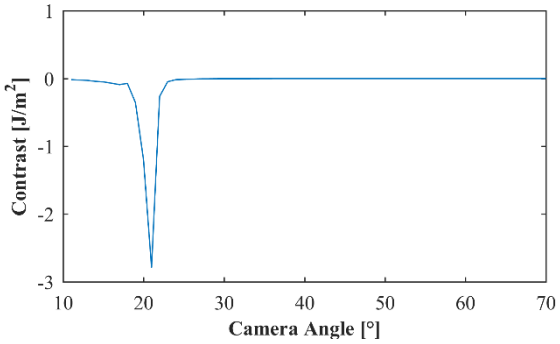

Figure 9. The average contrast between the black and white modules of S5 from different viewing angles.

It can be seen that as the camera gradually approached the theoretical maximum reflection angle of 20°, the contrast increased, and then immediately decreased until it became completely zero. Interestingly, it could be seen that the black and white modules were still distinguishable on the sample over 40°, while the contrast became zero after 25°. This system verified the theoretical viewing angle (20°) for best contrast of the 10° features of the anisotropic surfaces. The measurement of contrast could be used to directly reflect the quality of the microstructures of the surface.

4. Conclusions

This article presents the diamond machining to create optical functional surfaces on RSA 905. The surface function was the contrast that produced by different orientated microstructures of the sample surface under a fixed light source.

The surface microstructure geometry and burr height were measured and analysed to evaluate the quality of processing, while the quantitative measurement of surface function correlated the surface functionality and the quality of the microstructures. The width and depth of the microstructure were correlated and the variation of the ratio between the two dimensions was caused by the vibration of the tool in the z-axis direction. The vibration also caused the micro-ridge surface fluctuations, which would affect the surface function.

Future work will be dedicated to the improvement of the surface roughness measurement of the large slope angle of microstructures by the confocal measurement. The evaluation of the optical functionality of microstructured surface with large surface angle still needs to be optimized.

References

[1] Kasemo, Bengt. "Biological surface science." Surface science 500.1-3 (2002): 656-677.

[2] Ding, Changqin, Anwei Zhu, and Yang Tian. "Functional surface engineering of C-dots for fluorescent biosensing and in vivo bioimaging." Accounts of chemical research 47.1 (2013): 20-30.

[3] Haas-Santo, K., M. Fichtner, and K. Schubert. "Preparation of microstructure compatible porous supports by sol–gel synthesis for catalyst coatings." Applied Catalysis A: General 220.1-2 (2001): 79-92.

[4] Van Ostrand, Dan, Carey King, and Garth Gobell. "Optical microstructures for light extraction and control." U.S. Patent No. 7,486,854. 3 Feb. 2009.

[5] Montemor, M. F. "Functional and smart coatings for corrosion protection: a review of recent advances." Surface and Coatings Technology 258 (2014): 17-37.

[6] M'Saoubi, R., et al. "A review of surface integrity in machining and its impact on functional performance and life of machined products." International Journal of Sustainable Manufacturing 1.1-2 (2008): 203-236.

[7] Huang, Rui, et al. "Ultra-precision machining of radial Fresnel lens on roller moulds." CIRP Annals 64.1 (2015): 121-124.

[8] Li, C. J., et al. "Ultra-precision machining of Fresnel lens mould by single-point diamond turning based on axis B rotation." The International Journal of Advanced Manufacturing Technology 77.5-8 (2015): 907-913.

[9] Zhang, XinQuan, et al. "Diamond micro engraving of gravure roller mould for roll-to-roll printing of fine line electronics." Journal of Materials Processing Technology 225 (2015): 337-346.

[10] Brinksmeier, Ekkard, and Lars Schönemann. "Generation of discontinuous microstructures by diamond micro chiseling." CIRP Annals 63.1 (2014): 49-52.

[11] Fang, F. Z., et al. "Manufacturing and measurement of freeform optics." CIRP Annals 62.2 (2013): 823-846.

[12] Li, Dongya, et al. "On the effect of machining strategy in micro milling of tool steel surface micro features with optical functionality." Euspen Special Interest Group Meeting 2018: Structured & Freeform Surfaces. 2018.

[13] Li, Dongya, et al. "Evaluation of optical functional surfaces on the injection moulding insert by micro milling process." euspen Special Interest Group Meeting: Micro/Nano Manufacturing. The European Society for Precision Engineering and Nanotechnology, 2017.

[14] Regi, Francesco, et al. "A method for the characterization of the reflectance of anisotropic functional surfaces." Surface Topography: Metrology and Properties 6.3 (2018): 034005.

[15] http://www.nanotechsys.com/

[16] http://www.rsp-technology.com/

[17] https://contour-diamonds.com/

[18] Quagliotti, D., Baruffi, F., Tosello, G., Gasparin, S., Annoni, M., Parenti, P., Sobiecki, R. and Hansen, H.N., 2016. Performance verification of focus variation and confocal microscopes measuring tilted ultra-fine surfaces. In euspen's 16th International Conference & Exhibition.